

## Extended TeV Halos May Commonly Exist around Middle-Aged Pulsars

A. Albert<sup>1</sup>, R. Alfaro<sup>2</sup>, C. Alvarez<sup>3</sup>, J. C. Arteaga-Velázquez<sup>4</sup>, D. Avila Rojas<sup>1,2</sup>, H. A. Ayala Solares<sup>1,5</sup>, R. Babu<sup>6</sup>, E. Belmont-Moreno<sup>1,2</sup>, A. Bernal<sup>7</sup>, K. S. Caballero-Mora<sup>1,3</sup>, T. Capistrán<sup>8</sup>, A. Carramiñana<sup>9</sup>, S. Casanova<sup>10</sup>, U. Cotti<sup>4</sup>, J. Cotzomi<sup>11</sup>, S. Coutiño de León<sup>12,13,\*</sup>, E. De la Fuente<sup>14</sup>, C. de León<sup>4</sup>, D. Depaoli<sup>15</sup>, P. Desiati<sup>12</sup>, N. Di Lalla<sup>16</sup>, R. Diaz Hernandez<sup>9</sup>, B. L. Dingus<sup>1</sup>, M. A. DuVernois<sup>12</sup>, J. C. Díaz-Vélez<sup>12</sup>, K. Engel<sup>17</sup>, C. Espinoza<sup>1,2</sup>, K. L. Fan<sup>17</sup>, K. Fang<sup>12,†</sup>, N. Fraija<sup>7</sup>, J. A. García-González<sup>18</sup>, F. Garfias<sup>7</sup>, H. Goksu<sup>15</sup>, M. M. González<sup>7</sup>, J. A. Goodman<sup>17</sup>, S. Groetsch<sup>6</sup>, J. P. Harding<sup>1</sup>, S. Hernández-Cadena<sup>2</sup>, I. Herzog<sup>19</sup>, D. Huang<sup>17</sup>, F. Hueyotl-Zahuantitla<sup>3</sup>, A. Iriarte<sup>7</sup>, S. Kaufmann<sup>20</sup>, D. Kieda<sup>21</sup>, J. Lee<sup>22</sup>, H. León Vargas<sup>2</sup>, J. T. Linnemann<sup>19</sup>, A. L. Longinotti<sup>7</sup>, G. Luis-Raya<sup>20</sup>, K. Malone<sup>1</sup>, O. Martínez<sup>11</sup>, J. Martínez-Castro<sup>23</sup>, J. A. Matthews<sup>24</sup>, P. Miranda-Romagnoli<sup>25</sup>, J. A. Morales-Soto<sup>4</sup>, E. Moreno<sup>11</sup>, M. Mostafá<sup>26</sup>, L. Nellen<sup>27</sup>, M. U. Nisa<sup>19</sup>, N. Omodei<sup>16</sup>, Y. Pérez Araujo<sup>2</sup>, E. G. Pérez-Pérez<sup>20</sup>, C. D. Rho<sup>28</sup>, D. Rosa-González<sup>9</sup>, E. Ruiz-Velasco<sup>15</sup>, H. Salazar<sup>11</sup>, D. Salazar-Gallegos<sup>19</sup>, A. Sandoval<sup>2</sup>, M. Schneider<sup>17</sup>, J. Serna-Franco<sup>2</sup>, Y. Son<sup>22</sup>, R. W. Springer<sup>21</sup>, O. Tibolla<sup>20</sup>, K. Tollefson<sup>19</sup>, I. Torres<sup>9</sup>, R. Torres-Escobedo<sup>29</sup>, R. Turner<sup>6</sup>, F. Ureña-Mena<sup>9</sup>, E. Varela<sup>11</sup>, L. Villaseñor<sup>11</sup>, X. Wang<sup>6</sup>, E. Willox<sup>17</sup>, H. Wu<sup>12,‡</sup> and H. Zhou<sup>29</sup>

<sup>1</sup>Los Alamos National Laboratory, Los Alamos, New Mexico, USA

<sup>2</sup>Instituto de Física, Universidad Nacional Autónoma de México, Ciudad de México, México

<sup>3</sup>Universidad Autónoma de Chiapas, Tuxtla Gutiérrez, Chiapas, México

<sup>4</sup>Universidad Michoacana de San Nicolás de Hidalgo, Morelia, México

<sup>5</sup>Department of Physics, Pennsylvania State University, University Park, Pennsylvania, USA

<sup>6</sup>Department of Physics, Michigan Technological University, Houghton, Michigan, USA

<sup>7</sup>Instituto de Astronomía, Universidad Nacional Autónoma de México, Ciudad de México, México

<sup>8</sup>Università degli Studi di Torino, I-10125 Torino, Italy

<sup>9</sup>Instituto Nacional de Astrofísica, Óptica y Electrónica, Puebla, México

<sup>10</sup>Instytut Fizyki Jadrowej im Henryka Niewodniczanskiego Polskiej Akademii Nauk, IFJ-PAN, Krakow, Poland

<sup>11</sup>Facultad de Ciencias Físico Matemáticas, Benemérita Universidad Autónoma de Puebla, Puebla, México

<sup>12</sup>Department of Physics, University of Wisconsin—Madison, Madison, Wisconsin, USA

<sup>13</sup>Instituto de Física Corpuscular, CSIC, Universitat de València, E-46980, Paterna, Valencia, Spain

<sup>14</sup>Departamento de Física, Centro Universitario de Ciencias Exactas e Ingenierías, Universidad de Guadalajara, Guadalajara, México

<sup>15</sup>Max-Planck Institute for Nuclear Physics, 69117 Heidelberg, Germany

<sup>16</sup>Department of Physics, Stanford University, Stanford, California 94305-4060, USA

<sup>17</sup>Department of Physics, University of Maryland, College Park, Maryland, USA

<sup>18</sup>Tecnológico de Monterrey, Escuela de Ingeniería y Ciencias, Ave. Eugenio Garza Sada 2501, N.L., Monterrey, 64849, México

<sup>19</sup>Department of Physics and Astronomy, Michigan State University, East Lansing, Michigan, USA

<sup>20</sup>Universidad Politécnica de Pachuca, Pachuca, Hgo, México

<sup>21</sup>Department of Physics and Astronomy, University of Utah, Salt Lake City, Utah, USA

<sup>22</sup>University of Seoul, Seoul, Republic of Korea

<sup>23</sup>Centro de Investigación en Computación, Instituto Politécnico Nacional, México City, México

<sup>24</sup>Department of Physics and Astronomy, University of New Mexico, Albuquerque, New Mexico, USA

<sup>25</sup>Universidad Autónoma del Estado de Hidalgo, Pachuca, México

<sup>26</sup>Department of Physics, Temple University, Philadelphia, Pennsylvania, USA

<sup>27</sup>Instituto de Ciencias Nucleares, Universidad Nacional Autónoma de México, Ciudad de México, México

<sup>28</sup>Department of Physics, Sungkyunkwan University, Suwon 16419, South Korea

<sup>29</sup>Tsung-Dao Lee Institute, Shanghai Jiao Tong University, Shanghai, China



(Received 10 July 2024; revised 14 January 2025; accepted 11 March 2025; published 30 April 2025)

Extended gamma-ray emission around isolated pulsars at TeV energies, also known as TeV halos, have been found around a handful of middle-aged pulsars. The halos are significantly more extended than their pulsar wind nebulae but much smaller than the particle diffusion length in the interstellar medium. The origin of TeV halos is unknown. Interpretations invoke either local effects related to the environment of a

\* Contact author: scoutino@ific.uv.es

† Contact author: kefang@physics.wisc.edu

‡ Contact author: hwu298@wisc.edu

pulsar or generic particle transport behaviors. The latter scenario predicts that TeV halos would be a universal phenomena for all pulsars. We searched for extended gamma-ray emission around 36 isolated middle-aged pulsars identified by radio and gamma-ray facilities using 2321 days of data from the High-Altitude Water Cherenkov (HAWC) Observatory. Through a stacking analysis comparing TeV flux models against a background-only hypothesis, we identified TeV halolike emission at a significance level of  $5.10\sigma$ . Our results imply that extended TeV gamma-ray halos may commonly exist around middle-aged pulsars. This reveals a previously unknown feature about pulsars and opens a new window to identify the pulsar population that is invisible to radio, x-ray, and GeV gamma-ray observations.

DOI: [10.1103/PhysRevLett.134.171005](https://doi.org/10.1103/PhysRevLett.134.171005)

Gamma-ray emission with angular size of a few degrees was first detected by the High-Altitude Water Cherenkov (HAWC) Observatory around two nearby middle-aged energetic pulsars between 8 and 40 TeV in 2017 [1]. The TeV emission seen around those pulsars is much more extended than the pulsar wind nebulae whose sizes are no more than a few arc minutes [2–5]. These extended sources were named TeV halos [6]. Since the discovery of the first two TeV halos, more similar sources have been identified by HAWC [7] and LHAASO [8]. To date, the online catalog for TeV Astronomy (TeVCat [9]) reports a total of about ten TeV halos and TeV halo candidates. Counterparts of TeV halos at lower energies have been found in *Fermi*-LAT [5,10] and H.E.S.S. [4] data.

The origin of the TeV halos is largely unknown [11]. The emission cannot be explained by electron diffusion in the interstellar medium (ISM) as it requires a suppression of the cosmic-ray diffusivity by 100–1000 times [1]. Several explanations have been proposed, but all have weaknesses. Models can be divided into two main classes, attributing the slow diffusion to a turbulence that universally exists around the central source [12,13] or preexisting regions of non-standard relativistic electron transport [14,15]. A related debate is whether the halos commonly exist around middle-aged pulsars [16] or most middle-aged pulsars do not develop halos [17].

The several known TeV halos present similar physical extensions [6], which are related to the cooling time of very-high-energy (0.1–100 TeV) electrons in the cosmic microwave background (CMB) and interstellar radiation field. The flux of the TeV emission seems to be related to the pulsar’s emissivity [18]. Motivated by the similarity of the known sources, we perform the first systematic search for TeV halos in the HAWC data around pulsar populations that are identified by radio and GeV gamma-ray observations.

*Samples of isolated middle-aged pulsars*—Our analysis uses radio pulsars from the Australia Telescope National Facility (ATNF) catalog [19,20] and gamma-ray pulsars from the Third LAT Pulsar catalog (3PC) [21]. We apply the following selection criteria: (1) a pulsar is in HAWC’s field of view ( $-26^\circ < \delta < 64^\circ$ ), (2) not in a binary system, (3) middle aged, defined as the spin down age  $P/(2\dot{P}) > 20$  kyr, where  $P$  and  $\dot{P}$  are the barycentric

period of the pulsar and its time derivative, respectively, and (4) with the spin-down flux above the HAWC sensitivity. The spin-down flux is defined as  $\dot{E}/(4\pi d^2)$ , where  $\dot{E}$  and  $d$  are the spin-down power and distance, respectively. A total of 1304 sources pass the first three selection criteria. Since the distance to a pulsar is needed to estimate its detectability and the angular size of its halo, we remove 3 pulsars without reported distances from the list. After applying the fourth criterion, the selection yields a total of 86 sources, including 49 gamma-ray pulsars and 72 radio-loud pulsars. Among the gamma-ray pulsars, 14 are radio quiet and mutually exclusive from the radio-loud sample.

Some of the sources are located in highly populated regions of TeV gamma-ray sources. To avoid source confusion, we further removed pulsars within  $2^\circ.5$  of the TeVCat sources that are not classified as a TeV halo or TeV halo candidate. The choice of  $2^\circ.5$  makes sure that the contamination from most TeV sources is avoided while the sample remains sufficiently large. Our final sample has 36 isolated middle-aged pulsars, including 24 gamma-ray pulsars and 24 radio-loud pulsars (12 pulsars are both radio-loud and gamma-ray bright). Among them, 28 pulsars have not been associated with a known TeV halo or TeV halo candidate. Figure 1 shows a HAWC significance map of the entire sky above 300 GeV in Galactic coordinates, overlaying the positions of the pulsars used in the analysis. Detailed properties of the pulsars are presented in Supplemental Material [22].

*HAWC data*—HAWC is a gamma-ray and cosmic-ray observatory located near Puebla, Mexico at an altitude of 4,100 meters. This analysis uses the HAWC Data Pass 5 [23] with 2321 days of exposure. The gamma-ray energy is estimated using the fraction of the photomultiplier tubes (PMTs) that are triggered in each shower event, called  $f_{\text{Hit}}$  bins [24].

*Stacking analysis*—Motivated by the similarity of the observed TeV halos, we combine the observations of the pulsar population accessible to HAWC to constrain the common factors that impact the gamma-ray production in TeV halos.

We model the TeV halo emission of the  $i$ th pulsar in the source list with a spatial model and a spectral model. The spatial model is a Gaussian template with an extension  $\sigma$

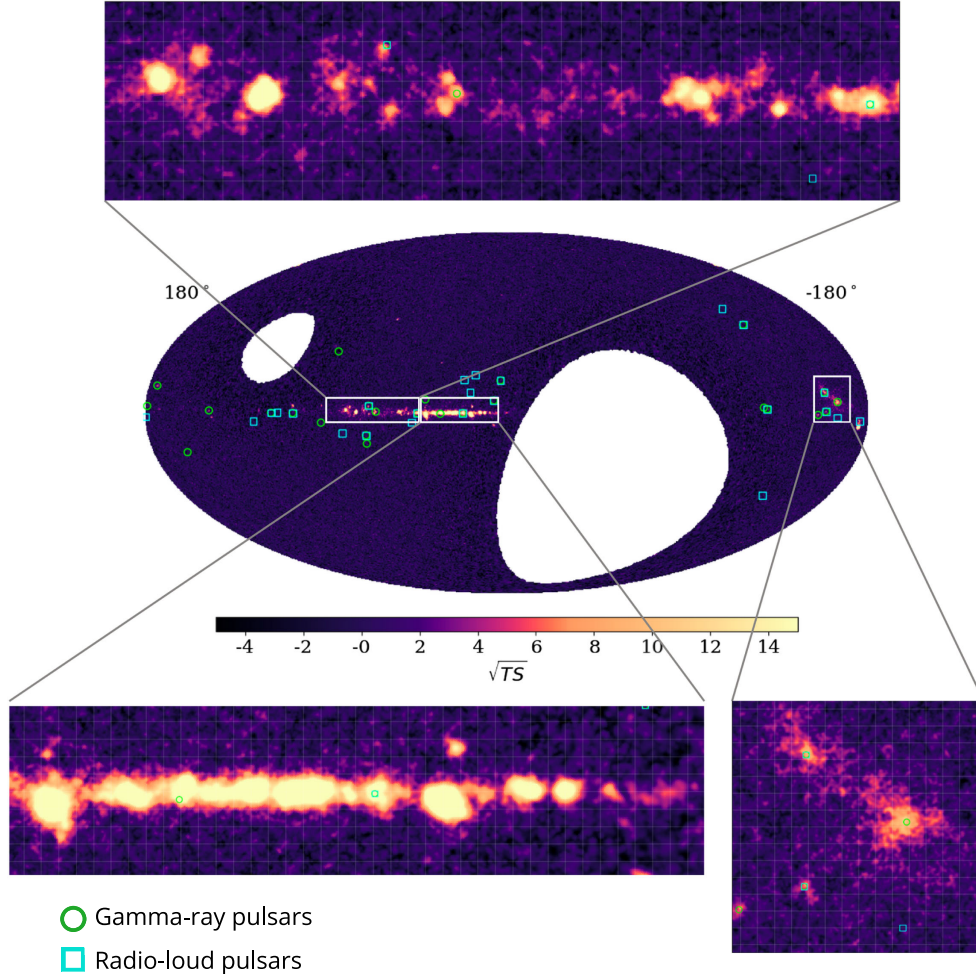


FIG. 1. Significance map of the gamma-ray sky observed by HAWC based on 2321 days of data, between 300 GeV and  $\sim 100$  TeV. The green circles and cyan squares indicate the positions of the 24 gamma-ray pulsars and 24 radio pulsars used in this analysis, respectively. Among them, 12 pulsars are both gamma ray bright and radio loud.

scaled to the extension of the Geminga TeV halo,  $\sigma_i = \sigma_{\text{Geminga}}(d_{\text{Geminga}}/d_i)$ , where  $\sigma_{\text{Geminga}} = 2^\circ$  [6],  $d_{\text{Geminga}} = 0.25$  kpc and  $d_i$  is the distance to the pulsar in kpc. The value of  $\sigma_i$  is fixed in the fit. The spectral model describes the flux as a simple power law,  $dN/dEdAdt \propto (E/E_{\text{piv}})^{-\alpha}$ , where  $E_{\text{piv}}$  is the pivot energy and  $\alpha$  is the spectral index. We fit such a model to data in both the full energy range, 0.316 TeV–100 TeV, and in half-decade bins. In the full energy range the pivot energy is fixed to 30 TeV, while in the fit in each energy bin, the pivot energy is chosen to be the median energy of each energy bin. We fix the spectral index to  $\alpha = 2.7$  and evaluate the uncertainties associated with the choices of spatial extension and spectral index later in a systematic study.

We assume that all TeV halos in the population may be described by the same physics, where the differential energy flux of a TeV halo,  $F_i \equiv E^2(dN/dEdAdt)_i$ , is scaled to the available power of a pulsar,  $A_i$ , through a common efficiency,  $\eta$ :  $F_i = \eta A_i$ . The efficiency  $\eta$  represents the fraction of the pulsar's power that is converted

into the differential TeV halo luminosity at a given energy. We consider two scenarios for  $A_i$ , namely, the spin-down flux scenario and the GeV flux scenario. In the former model,  $A_i = \dot{E}_i/(4\pi d_i^2)$ , where  $\dot{E}_i = 4\pi^2 I \dot{P}_i P_i^{-3}$  is the current-day spin-down power with  $I = 10^{45}$  g cm $^{-2}$  being the moment of inertia of a neutron star which is fixed to be the same for all pulsars. In this scenario, the closer and more energetic pulsars have a higher gamma-ray flux. In the GeV flux scenario, we assume  $A_i = F_{0.1-100 \text{ GeV}}$ , where  $F_{0.1-100 \text{ GeV}}$  is the integrated flux of the pulsar between 100 MeV and 100 GeV provided by 3PC. In this second scenario, brighter GeV pulsars would produce brighter very-high energy (VHE) gamma-ray halos. Independent of the distance, the spin-down flux and the GeV flux are correlated, though the slope has a large dispersion as shown in Ref. [21]. We therefore treat them as two separate scenarios in the stacking analysis.

We fit each source in the pulsar samples using the spectral and spatial model described above. We then add

their log-likelihood profiles to constrain the common efficiency  $\eta$  in each power scenario and energy bin.

We compare the combined signal with a null hypothesis, where the flux of extended TeV halo emission around pulsars is consistent with background fluctuations. We first construct a test statistic (TS), which is defined to be twice the logarithm of the ratio of the likelihoods when fitting the data with and without TeV halos around the selected pulsars,  $TS \equiv 2 \ln[\mathcal{L}(\hat{\eta})/\mathcal{L}(\eta = 0)]$ . To understand the TS distribution of the null hypothesis, we perform a Monte Carlo simulation to generate random positions based on the spatial distribution of Galactic pulsars (see Supplemental Material for details regarding the background source generation). These positions are treated as fake sources and we stack their likelihood profiles in the actual data. We use the same selection criteria as for the real sources to form a fake source sample, that is, a fake source needs to be in the HAWC field of view and located at least  $2^\circ.5$  away from TeVCat sources. The black curve in the left panel of Fig. 2 presents the distribution of the TS under the null hypothesis. Out of 101 965 trials of stackings of 10 fake sources, the highest TS is found to be  $TS_{bg} = 69.5$ . Therefore, a TS much higher than  $TS_{bg}$  can safely reject the background hypothesis at least at the level of  $4.27\sigma$ . We verified that the background TS distribution is not sensitively impacted by the number of stacked sources (see Supplemental Material). The background TS distribution departs from a Chi-square over two ( $\chi^2/2$ ) distribution that is expected from Wilks' theorem [25]. This is caused by the fake sources that land at the outskirts of TeV sources that

are more extended than  $2^\circ.5$ , the separation threshold adopted in our source selection criteria.

*Results*—We perform the stacking analysis using radio and gamma-ray pulsar samples and the full energy range. We adopt the spin-down flux scenario for radio pulsars, considering that not all radio pulsars are detected in GeV gamma rays. For gamma-ray pulsars, we consider both weighting scenarios. This led to a total of 3 trials of stacking analyses. To avoid bias caused by bright TeV halos, we first consider the subsample that is not associated with known TeV halo or TeV halo candidates, which includes 17 gamma-ray and 20 radio-loud pulsars. The highest TS is found to be  $TS = 108$ , obtained from the trial using gamma-ray pulsars and the spin-down flux scenario. Based on an extrapolation of the simulated background TS distribution (gray curve in left panel of Fig. 2), this TS value corresponds to a  $p$  value  $p = 5.5 \times 10^{-8}$ , based on an extrapolation of the TS distribution of the background trials.

The other two trials result in  $TS = 92$  and  $96$ , respectively, as also indicated in the figure. We apply a penalty trial factor to account for the fact that multiple trials may increase the possibility of finding a significant event. Although the three signal hypotheses are correlated, we account for a conservative trial factor of 3 when evaluating a post-trials  $p$  value. Specifically, we multiply the lowest  $p$  value by 3 to obtain a post-trial  $p$  value and convert the  $p$  value to a Gaussian significance of  $5.10\sigma$ . This positive detection of extended TeV gamma-ray emission around pulsar populations not previously associated with TeV

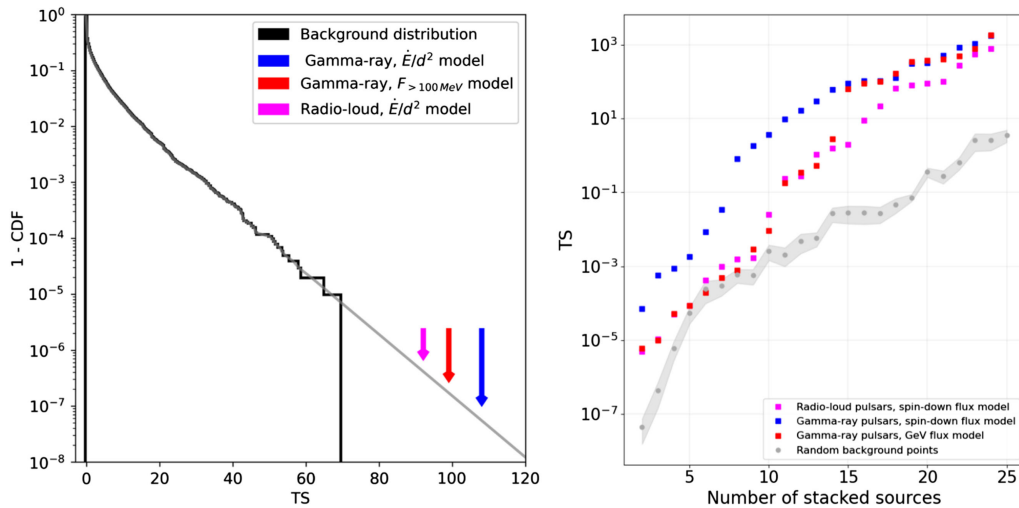


FIG. 2. Left: test statistics (TS) of the stacked likelihoods using radio and gamma-ray pulsars. The black steps indicate the cumulative distribution function of the stacked TS values obtained from samples consisting of random positions. The gray curve is an extrapolation based on the 101 965 trials of background samples. The arrows indicate the results of analyses using different pulsar groups and weighting schemes. Right: TS values resulted from stacking analyses in the full energy range as a function of the number of stacked sources. From right to left, the sources with the highest TS are removed from the sample one by one. Colors indicate the pulsar samples and weighting schemes. The gray shaded region indicates the mean and standard deviation found from the same analysis but with background samples consisting of random positions.

halos indicates that TeV halos may commonly exist around middle-aged pulsars.

To ensure that the stacked TS is not dominantly contributed by a few bright sources, we gradually remove the sources with the highest TS values from a pulsar sample and examine the evolution of the stacked TS values. We use all pulsars including those associated with known TeV halos in this test. The right panel of Fig. 2 shows that in all weighting scenarios and pulsar groups, the stacked TS gradually declines as the number of stacked sources decreases. The trend cannot be explained by the background which is indicated by the gray shaded region. The evidence of an excess halo emission against the background comes from the entire pulsar population as opposed to just the brightest sources.

Finally, to examine whether the emission is physically extended, we perform the stacking analysis using a point-like spatial template. Similar to the extended-model analysis, we confine the efficiency parameter using a combined likelihood. We compare the two spatial models based on the TS values and the Bayesian information criterion (BIC) from the analysis using the full energy range. We find that in all weighting scenarios and pulsar groups, the extended model is significantly preferred [26] over the pointlike model with  $TS_{\text{extended}} - TS_{\text{point}} > 25$  and  $BIC_{\text{point}} - BIC_{\text{extended}} > 10$ .

The halo efficiencies computed using all pulsars are generally consistent with those from pulsars not associated with known TeV halos within uncertainties as shown in Fig. 6 in Supplemental Material. The systematic uncertainties include the effects due to spectral models, extension models, as well as uncertainties in our detector configurations. See Supplemental Material for details regarding the evaluation of the systematic errors. The efficiencies decrease as a function of the photon energy because the gamma-ray spectrum follows a power-law distribution. On average, the differential energy flux in TeV halos is at the level of (0.01–1)% of the spin-down flux. For gamma-ray pulsars, the energy deposited in TeV halos ranges from (0.1–10)% of that in the GeV emission of the pulsars.

*Implications of commonly existing TeV halos*—We have used a stacking technique that combines the likelihood profiles of radio and gamma-ray pulsars accessible to HAWC to test the hypothesis that the flux of extended TeV halo emission around pulsars is consistent with background fluctuations. Our analysis has assumed that the TeV flux of a pulsar halo scales with the spin-down flux or the GeV gamma-ray flux of the pulsar. Using pulsars that have not been associated with a known TeV halo, the null hypothesis is rejected at the level of  $5.10\sigma$ .

Our analysis implies an existence of ubiquitous TeV halos around isolated middle-aged pulsars. This establishes TeV halos as a new pulsar phenomenon that has a distinct origin from pulsar wind nebulae, as the latter are usually orders of magnitude more compact for pulsars at this age.

A common existence of TeV halos suggests that the production mechanism of TeV halos is more likely related to the transport of relativistic particles in the vicinity of a pulsar than the local environment of the observed halos. It also suggests a leptonic origin of the TeV gamma-ray emission since hadronic emission highly depends on the gas density (e.g., Ref. [27]) and would vary from pulsar to pulsar.

The longer confinement of relativistic electrons by the halos than the average ISM has strong implications for indirect searches for dark matter. While these halos provide an alternative way to explain the GeV excess in the Galactic center [28], they also make it harder to explain the cosmic-ray positron excess [29–31] with nearby pulsars [1,27,32], compared to scenarios involving exotic physics. A common existence of TeV halos also impacts the view of Galactic gamma-ray astronomy. These halos may contribute to the diffuse Galactic plane emission observed by Tibet AS $\gamma$  [33], HAWC [34], and LHAASO [35] experiments and explain the hardening of the diffuse  $\gamma$ -ray emission around 1 TeV [36–39].

Our Letter suggests that a conversion of the spin-down power to the TeV halo emission could be as efficient as  $\sim 0.1\%$  and that the power carried by a TeV halo is about 1% of that by the GeV magnetospheric emission at 10 TeV (see Fig. 6 in Supplemental Material). The spin-down flux model resulted in a higher TS than the GeV flux model, though the difference is not statistically significant. This could be related to the fact that the observation of GeV magnetospheric emission may be biased by orientation effects. We further extended this analysis to constrain the diffusion radius of electrons around our sample of TeV halos. From this, we derived a diffusion coefficient of  $D_0 \approx 2.0 \times 10^{27} \text{ cm}^2 \text{ s}^{-1}$  at a reference energy of  $E_0 = 10 \text{ GeV}$ , consistent with measurements around Geminga [1] (see Supplemental Material and Table IV for more details regarding the diffusion coefficient study). These results reinforce the idea that electron propagation in TeV halos occurs in a suppressed diffusion environment, significantly lower than the typical Galactic diffusion coefficient.

Future observations of the spatial profiles of individual halos over a wide energy range would be needed to understand how electrons diffuse in TeV halos. Wide-field gamma-ray detectors with better sensitivity and covering the southern sky can carry out such population studies [40]. Finally, while pulsars are typically identified via their pulsed emission in radio, x-ray, and GeV gamma-ray wavelengths, TeV halos open a new window on pulsar observations. In particular, they offer a unique way to probe the “invisible” pulsars [6] with beaming angles misaligned with observers and middle-aged and old pulsars with a surface density too low to be detected in other wavelengths.

*Acknowledgments*—We acknowledge support from the following: the US National Science Foundation (NSF); the

US Department of Energy Office of High-Energy Physics; the Laboratory Directed Research and Development (LDRD) program of Los Alamos National Laboratory; Consejo Nacional de Ciencia y Tecnología (CONACyT), México, Grant No. LNC-2023-117, No. 271051, No. 232656, No. 260378, No. 179588, No. 254964, No. 258865, No. 243290, No. 132197, No. A1-S-46288, No. A1-S-22784, No. CF-2023-I-645, cátedras 873, 1563, 341, 323, Red HAWC, México; DGAPA-UNAM Grant No. IG101323, No. IN111716-3, No. IN111419, No. IA102019, No. IN106521, No. IN114924, No. IN110521, No. IN102223; VIEP-BUAP; PIFI 2012, 2013, PROFOCIE 2014, 2015; the University of Wisconsin Alumni Research Foundation; the Institute of Geophysics, Planetary Physics, and Signatures at Los Alamos National Laboratory; Polish Science Centre Grant No. 2024/53/B/ST9/02671; Coordinación de la Investigación Científica de la Universidad Michoacana; Royal Society—Newton Advanced Fellowship 180385; Gobierno de España and European Union—NextGenerationEU, Grant No. CNS2023-144099; The Program Management Unit for Human Resources & Institutional Development, Research and Innovation, NXPO (Grant No. B16F630069); Coordinación General Académica e Innovación (CGAI-UdeG), PRODEP-SEP UDG-CA-499; Institute of Cosmic Ray Research (ICRR), University of Tokyo. H. F. acknowledges support by NASA under Award No. 80GSFC21M0002. C. R. acknowledges support from National Research Foundation of Korea (RS-2023-00280210). We also acknowledge the significant contributions over many years of Stefan Westerhoff, Gaurang Yodh, and Arnulfo Zepeda Domínguez, all deceased members of the HAWC Collaboration. Thanks to Scott Delay, Luciano Díaz, and Eduardo Murrieta for technical support.

[1] A. U. Abeysekara *et al.*, Extended gamma-ray sources around pulsars constrain the origin of the positron flux at Earth, *Science* **358**, 911 (2017).  
 [2] B. Posselt *et al.*, Geminga’s puzzling pulsar wind nebula, *Astrophys. J.* **835**, 66 (2017).  
 [3] L. Birzan, G. G. Pavlov, and O. Kargaltsev, Chandra observations of the elusive pulsar wind nebula around PSR B0656 + 14, *Astrophys. J.* **817**, 129 (2016).  
 [4] H. E. S. S. Collaboration *et al.*, Detection of extended  $\gamma$ -ray emission around the Geminga pulsar with H.E.S.S., *Astron. Astrophys.* **673**, A148 (2023).  
 [5] M. Di Mauro, S. Manconi, and F. Donato, Detection of a  $\gamma$ -ray halo around Geminga with the Fermi -LAT data and implications for the positron flux, *Phys. Rev. D* **100**, 123015 (2019); **104**, 089903(E) (2021).  
 [6] T. Linden, K. Auchettl, J. Bramante, I. Cholis, K. Fang, D. Hooper, T. Karwal, and S. W. Li, Using HAWC to discover invisible pulsars, *Phys. Rev. D* **96**, 103016 (2017).  
 [7] A. Albert *et al.*, 3HWC: The third HAWC catalog of very-high-energy gamma-ray sources, *Astrophys. J.* **905**, 76 (2020).

[8] F. Aharonian *et al.*, Extended very-high-energy gamma-ray emission surrounding PSR J0622 + 3749 observed by LHAASO-KM2A, *Phys. Rev. Lett.* **126**, 241103 (2021).  
 [9] <http://tevcat.uchicago.edu>  
 [10] S. Abdollahi, F. Acero, A. Acharyya, A. Adelfio, Ajello *et al.*, Search for extended GeV sources in the inner galactic plane, [arXiv:2411.07162](https://arxiv.org/abs/2411.07162).  
 [11] R. López-Coto, E. de Oña Wilhelmi, F. Aharonian, E. Amato, and J. Hinton, Gamma-ray haloes around pulsars as the key to understanding cosmic-ray transport in the Galaxy, *Nat. Astron.* **6**, 199 (2022).  
 [12] C. Evoli, T. Linden, and G. Morlino, Self-generated cosmic-ray confinement in TeV halos: Implications for TeV  $\gamma$ -ray emission and the positron excess, *Phys. Rev. D* **98**, 063017 (2018).  
 [13] P. Mukhopadhyay and T. Linden, Self-generated cosmic-ray turbulence can explain the morphology of TeV halos, *Phys. Rev. D* **105**, 123008 (2022).  
 [14] R.-Y. Liu, H. Yan, and H. Zhang, Understanding the multiwavelength observation of Geminga’s TeV halo: The role of anisotropic diffusion of particles, *Phys. Rev. Lett.* **123**, 221103 (2019).  
 [15] P. De La Torre Luque, O. Fornieri, and T. Linden, Anisotropic diffusion cannot explain TeV halo observations, *Phys. Rev. D* **106**, 123033 (2022).  
 [16] T. Sudoh, T. Linden, and J. F. Beacom, TeV halos are everywhere: Prospects for new discoveries, *Phys. Rev. D* **100**, 043016 (2019).  
 [17] P. Martin, A. Marcowith, and L. Tibaldo, Are pulsar halos rare?. Modeling the halos around PSRs J0633 + 1746 and B0656 + 14 in the light of Fermi-LAT, HAWC, and AMS-02 observations and extrapolating to other nearby pulsars, *Astron. Astrophys.* **665**, A132 (2022).  
 [18] M. Di Mauro, S. Manconi, and F. Donato, Evidences of low-diffusion bubbles around Galactic pulsars, *Phys. Rev. D* **101**, 103035 (2020).  
 [19] <http://www.atnf.csiro.au/research/pulsar/psrcat>—version 1.71.  
 [20] R. N. Manchester, G. B. Hobbs, A. Teoh, and M. Hobbs, The Australia Telescope National Facility Pulsar Catalogue, *Astron. J.* **129**, 1993 (2005).  
 [21] D. A. Smith *et al.*, The third Fermi Large Area Telescope catalog of gamma-ray pulsars, *Astrophys. J.* **958**, 191 (2023).  
 [22] See Supplemental Material at <http://link.aps.org/supplemental/10.1103/PhysRevLett.134.171005> for properties of pulsars, background test statistic distribution, likelihood analysis, halo efficiencies, systematic uncertainties, diffusion coefficient calculation and the list of sources.  
 [23] A. Albert *et al.*, Performance of the HAWC observatory and TeV gamma-ray measurements of the Crab Nebula with improved extensive air shower reconstruction algorithms, *Astrophys. J.* **972**, 144 (2024).  
 [24] A. U. Abeysekara *et al.*, Observation of the Crab Nebula with the HAWC gamma-ray observatory, *Astrophys. J.* **843**, 39 (2017).  
 [25] S. S. Wilks, The large-sample distribution of the likelihood ratio for testing composite hypotheses, *Ann. Math. Stat.* **9**, 60 (1938).

- [26] R. E. Kass and A. E. Raftery, Bayes factors, *J. Am. Stat. Assoc.* **90**, 773 (1995).
- [27] B. Schroer, C. Evoli, and P. Blasi, TeV halos and the role of pulsar wind nebulae as sources of cosmic-ray positrons, *Phys. Rev. D* **107**, 123020 (2023).
- [28] D. Hooper and T. Linden, Millisecond pulsars, TeV halos, and implications for the Galactic Center gamma-ray excess, *Phys. Rev. D* **98**, 043005 (2018).
- [29] O. Adriani *et al.* (PAMELA Collaboration), An anomalous positron abundance in cosmic rays with energies 1.5–100 GeV, *Nature (London)* **458**, 607 (2009).
- [30] M. Ackermann *et al.*, Measurement of separate cosmic-ray electron and positron spectra with the Fermi Large Area Telescope, *Phys. Rev. Lett.* **108**, 011103 (2012).
- [31] M. Aguilar *et al.* (AMS Collaboration), Towards understanding the origin of cosmic-ray positrons, *Phys. Rev. Lett.* **122**, 041102 (2019).
- [32] S. Manconi, M. Di Mauro, and F. Donato, Contribution of pulsars to cosmic-ray positrons in light of recent observation of inverse-Compton halos, *Phys. Rev. D* **102**, 023015 (2020).
- [33] M. Amenomori *et al.* (Tibet ASgamma Collaboration), First detection of sub-PeV diffuse gamma rays from the galactic disk: Evidence for ubiquitous galactic cosmic rays beyond PeV energies, *Phys. Rev. Lett.* **126**, 141101 (2021).
- [34] A. U. Abeysekara *et al.* (HAWC Collaboration), Galactic gamma-ray diffuse emission at TeV energies with HAWC data, *Proc. Sci., ICRC2021* (**2021**) 835.
- [35] Z. Cao *et al.*, Measurement of ultra-high-energy diffuse gamma-ray emission of the Galactic plane from 10 TeV to 1 PeV with LHAASO-KM2A, *Phys. Rev. Lett.* **131**, 151001 (2023).
- [36] T. Linden and B. J. Buckman, Pulsar TeV halos explain the diffuse TeV excess observed by Milagro, *Phys. Rev. Lett.* **120**, 121101 (2018).
- [37] V. Vecchiotti, F. Zuccarini, F. L. Villante, and G. Pagliaroli, Unresolved sources naturally contribute to PeV gamma-ray diffuse emission observed by Tibet AS $\gamma$ , *Astrophys. J.* **928**, 19 (2022).
- [38] A. Dekker, I. Holst, D. Hooper, G. Leone, E. Simon, and H. Xiao, Diffuse ultra-high-energy gamma-ray emission from TeV halos, *Phys. Rev. D* **109**, 083026 (2024).
- [39] K. Fang, J. S. Gallagher, and F. Halzen, Milky Way as a neutrino desert: Implications of the IceCube galactic diffuse neutrino emission, *Nat. Astron.* **8**, 241 (2024).
- [40] P. Huentemeyer, S. BenZvi, B. Dingus, H. Fleischhack, H. Schoorlemmer, and T. Weisgarber, The Southern Wide-Field Gamma-Ray Observatory (SWGRO): A next-generation ground-based survey instrument, *Bull. Am. Astron. Soc.* **51**, 109 (2019); P. Abreu *et al.*, [arXiv:1907.07737](https://arxiv.org/abs/1907.07737).